# The Radio Frequency System for the MPET and EBIT

TITAN Group, TRIUMF

Nikolina Ilic
in collaboration with Chris Owen

December 21, 2007

SUMMARY ... 4

INTRODUCTION ... 5

About TITAN ... 5

The MPET ... 6
1. Motivation For Mass Measurements ... 6
2. Description of MPET and Mass Measurements ... 6
3. Electrode Arrangement ... 7
4. The RF System Summary ... 8

The EBIT ... 10
1. Motivation for Beta Spectroscopy ... 10
2. Description of EBIT and Beta Spectroscopy ... 10
3. Electrode Arrangement ... 12
5. RF System Summary ... 13
*A. Sideband Cooling* ... 13
*B. Rotating Wall Cooling* ... 14

THE RF SYSTEM ... 16

The MPET ... 16
1. The RF Generators ... 16
2. 180 Splitter Module ... 16
*A. The Circuit Design* ... 16
*B. The Mechanical Setup* ... 18
*C. The Digital Logic* ... 19
3. RF Amplifiers ... 21
*A. Specifications* ... 21
*B. Gain Control* ... 21
*D. Thermal Precautions* ... 22
*C. Power Supply* ... 22
*E. Mechanical Setup* ... 22
4. Terminations ... 23
5. Peak Diagnostic Detector ... 23
*A. The Circuit Design* ... 23
*B. Mechanical Setup* ... 24
6. DC Biasing Module ... 26
*A. The Circuit Design* ... 26
*B. The Mechanical Setup* ... 27

The EBIT ........................................................................................................ 28
1. Sideband Cooling Requirements............................................................ 28
2. Rotating Wall Cooling Requirements ..................................................... 29
3. Mechanical Considerations..................................................................... 30

CONCLUSION.................................................................................................... 31

Current Status and Future Development....................................................... 31
MPET.......................................................................................................... 31
EBIT........................................................................................................... 32

REFRENCES....................................................................................................... 33

APPENDICES ..................................................................................................... 34

| | |
|---|---|
| APPENDIX A | 0°/180° Splitter Module |
| APPENDIX B | DC Biasing Module |
| APPENDIX C | Diagnostic Detector |
| APPENDIX D | Mechanical Drawings |
| APPENDIX E | Datasheets |
| APPENDIX F | EBIT Cooling Calculations |

## SUMMARY

The TITAN facility at TRIUMF measures the masses of exotic fast-decaying nuclei with high precision. The experimental setup contains several traps which cool, bunch, charge-breed and trap ions. This document focuses on Radio Frequency systems for the Electron Beam Ion Trap (EBIT) and Measurement Penning Trap (MPET). A radio frequency is applied to certain electrodes in the two traps in order to excite the ions in a desirable manner.

The MPET uses a superposition of magnetic and electric fields in order to trap and measure the ions. The MPET measures masses with an uncertainty of $10^{-8}$ $\delta$m/m. When measuring masses, the EBIT is used to charge breed particles by knocking electrons out of their orbit using an electron gun. This charge-breeding allows the ion masses to be measured with greater resolution. The EBIT can also be used for other experiments such as Beta Spectroscopy and Fourier-tranform ion cyclotron resonance mass spectrometry.

In the MPET the radio frequency signals are applied to eight electrodes in dipole and azimuthal quadrupole configurations. The required frequency range is 100kHz to 70 MHz. The quadrupole configuration is responsible for coupling two of the eigenfrequencies of the ions. The dipole configuration is used in order to achieve mass selectivity.

In the EBIT the RF is applied in order to achieve sideband cooling or rotating wall cooling. Sideband cooling is applied at low densities where space charge effects can be neglected. Rotating wall cooling is applied at higher density where space charge effects are not negligible. Both types of cooling are used to decrease the size of the ion cloud trapped in the EBIT in order to observe it.

# INTRODUCTION

## About TITAN

TRIUMF's Ion Trap for Atomic and Nuclear (TITAN) science is located in the Isotope Separation and Acceleration (ISAC) facility at TRIUMF. Currently, TITAN's main goal is to measure masses of radioactive isotopes to within an uncertainty of $10^{-8}$ δm/m.

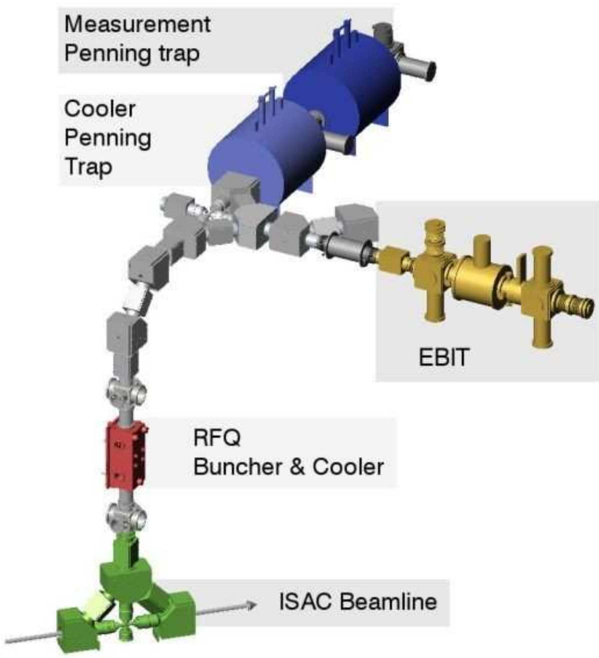


**Figure 1 – The Titan Setup**

The TITAN setup consists of several traps used to cool, charge-breed and trap radioactive isotopes. The diagram on the left shows the paths ions follow after they exit the ISAC Beamline. The TITAN Radio Frequency Quadrupole trap cools and bunches the incoming continuous beam of ions. The ions then enter the Electron Beam Ion Trap (EBIT), whose primary function is to increase the charge of the ions in order to get a better mass measurement resolution. In future experiments the EBIT may be used for to study EC branching ratios in order to correctly determine $\beta$-$\beta$- decay matrix elements. The Cooler Penning Trap (CPET) used cooling of highly charged ions, is yet to be installed. The final destination for the ions is the Mass Measurement Penning Trap, where ions are manipulated using radio frequency fields, and measured.

# The MPET

## 1. Motivation For Mass Measurements

There are many motivations for high precision mass measurements. The successful measurement of $^{11}Li$ that occurred in December 2007 is useful for studying the two-neutron separation energy. The two-neutron separation energy is the key parameter in a model, which might explain the halo nucleus structure of $^{11}Li$. Previous $^{11}Li$ mass measurements have not provided scientists with a precise and consistent number useful in determining this parameter.

Testing the unitarity of the Cabibbo-Kobayashi-Maskawa (CKM) matrix by measuring the mass of $^{74}Rb$ is another good physics motivation. The $V_{ud}$ matrix element can be obtained from the vector coupling constant, $G_v$, which can be obtained from the measurable ft value. Accurate measurements of $V_{ud}$ may help determine if CKM matrix is currently not unitary due to imprecise measurements or due to nature. The latter case might imply that there is more to physics than what the Standard Model presents.

## 2. Description of MPET and Mass Measurements

The Measurement Penning Trap (MPET) is where the high accuracy mass measurements of radioactive ions take place. The trap consists of two cap electrodes, and a middle ring electrode which has a hyperbolic cross section. The application of a weak electric field to these electrodes traps the ions in the Z-axis. Trapped in this axis, the ions oscillate with simple harmonic motion whose angular frequency is $\omega_z$. The electrodes sit insides a super conducting solenoid, which produces a strong magnetic field, trapping the ions in the remaining X and Y dimensions. In the X-Y plane the ions slowly drift around the trap axis with angular frequency $\omega_-$. The ions also exhibit reduced cyclotron motion, with angular frequency $\omega_+$. The reduced cyclotron motion is a fast motion around a small orbit due to the Lorenz force. The resulting three dimensional ion motion, shown in Figure 2 is a combination of the oscillatory motion, (frequency $\omega_z$ ) , the magnetron motion , (frequency $\omega_-$), and the

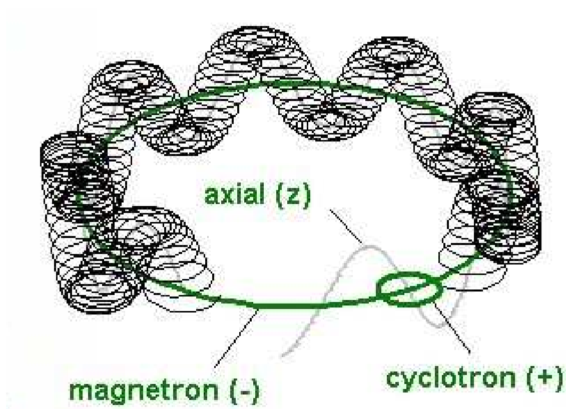

**Figure 2 – Motion of Ions in MPET**

cyclotron motion, (frequency $\omega_+$). The frequencies of these motions are called eigenfrequencies. The sum of the magnetron and reduced cyclotron eigenfrequnecies is equal to the cyclotron frequency of the ion:

$$\omega_+ + \omega_- = \omega_c = (q/m)*B$$

From the equation above, it is apparent that the mass of a particle can be obtained if the cyclotron frequency, the charge state, and the magnitude of the magnetic field are known. Since the charge state and magnetic field strength is known, the goal of the MPET is to measure the cyclotron frequency of the ions.

The magnetron and reduced cyclotron motions are coupled using azimuthal quadrupole Radio Frequency electric fields. The frequency of the applied RF field is close to that of the sum of the magnetron and reduced cyclotron frequencies. Coupling the two motions means that a periodic conversion from magnetron motion to cyclotron motion occurs.

After their motions are coupled, the ions are ejected from the trap and accelerated towards an MCP detector. The radial energy in the trap relates to the time of flight between the trap and the detector. On a time of flight versus RF frequency graph, the minimum corresponds to the cyclotron frequency, $\omega_c$. Using the $\omega_c$ value, the mass of the ions can then be calculated.

After the quadrupole field is applied, a Radio Frequency dipole field is applied in order to accomplish mass selectivity.

## 3. Electrode Arrangement

The penning trap electrodes are gold-coated copper. Parallel, 60cm long, 0.8 mm thick copper wires deliver voltages to the electrodes. The wires and electrodes are in a vacuum.

The arrangement of the Penning Trap Electrodes is shown in Figure 3. The electrodes are labeled according to what axis they sit on. The Z-axis points downstream of the beamline, the X-axis is horizontal, and the Y-axis is vertical. The X2+, Y2+, X2- and Y2- electrodes are separated from the X1+, Y1+, X1- and Y1- electrodes by the ring electrode.

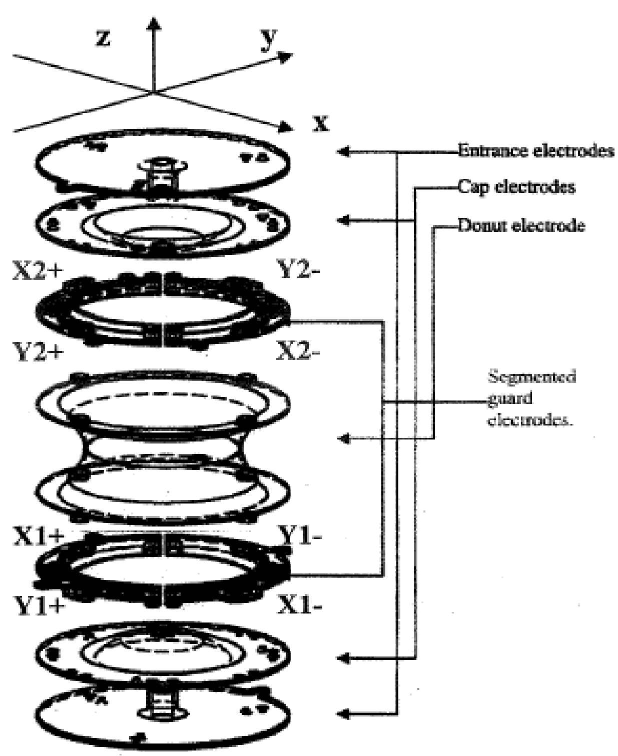


**Figure 3 – MPET Electrode Arrangement**

In order to generate the quadrupole and dipole fields described in the previous section, an RF is applied to the guard electrodes of the trap. These electrodes are also used for electric field corrections. In order to achieve the quadrupole or dipole field configuration in the center of trap, a combination of 0° and 180° phase RF fields must be applied to certain guard electrodes. Chart shows which RF configuration must be applied to the guard electrodes in order to get the desired excitation modes.

| ***Excitation Mode*** | ***RF phase on each electrode (°)*** | | | | | | | |
|---|---|---|---|---|---|---|---|---|
| | **1X-** | **1X+** | **1Y-** | **1Y+** | **2X-** | **2X+** | **2Y-** | **2Y+** |
| None | no RF | no RF | no RF | no RF | no RF | no RF | no RF | no RF |
| Dipole | no RF | no RF | 180 | 0 | no RF | no RF | 180 | 0 |
| Quadrupole | 0 | 0 | 180 | 180 | 0 | 0 | 180 | 180 |

**Table 1 – Configurations for dipole and quadrupole excitations**

## 4. The RF System Summary

A conceptual diagram of the Radio Frequency is shown in Figure 4. The radio frequency signal comes from two 80MHz Agilent function generators. One type of generator is set up for dipole excitation, while the other is set up for the subsequent quadrupole excitation.

A 3-way switch chooses the frequency on one of the two generators or selects a terminating 50Ω resistor. This switch is thus responsible for selecting the frequencies and switching the input signal from on to off and vice versa. Switching between on and off modes allows the switch to provide a pulse-mode radio frequency signal. The switch is controlled by logic described in subsequent sections.

The generated signal then goes to a device that splits it into a 0° phase and a 180° phase RF signal. The four 0° phase RF outputs are connected to four 3-way switches. Similarly the four 180° phase RF outputs are connected to the same four switches.

Each of the four 3-way switches is capable of selecting either a 0° phase RF signal, a 180° phase RF signal, or a 50Ω termination. The four 3-way switches are controlled by

DIP switches using logic described the Signal Logic sections. The DIP switches are set to two patterns, which correspond quadrupole and dipole excitation.

The signals are then amplified by 25W RF amplifiers from Amplifier Research. The amplifiers have a gain of +44dB. Varying the input signal at the source allows operators to control the output power, and thus amplitude. In order to balance the amplitude across the four different channels, the gains of each amplifier must be adjusted. This can be done by manually by turning a potentiometer on the Gain Control circuit.

There is a 50Ω resistor, which serves as a termination point after the amplifiers. The resistors are mounted onto a heat sink and cooled by fans. Before the termination, the voltages are sampled by a Diagnostic Detector. The detector provides a differential DC output which corresponds to RF peak-to peak values. This output goes through an Analog-to-Digital Converter into the Data Acquisition system.

The four channels coming out of the amplifiers connect to the DC Biasing Module, and provide it with 100kHz-70MHz RF signals. There are eight more inputs connected to the module, which provide 1kHz DC signals. The eight DC Biasing Module outputs connect to feedthough pins, which correspond to the eight guard electrodes inside the penning trap.  The outputs receive a superposition of high-frequency and low frequency signals from the inputs.  Filters found on the DC Biasing circuit board separate the high-frequency RF and DC signals from each other.

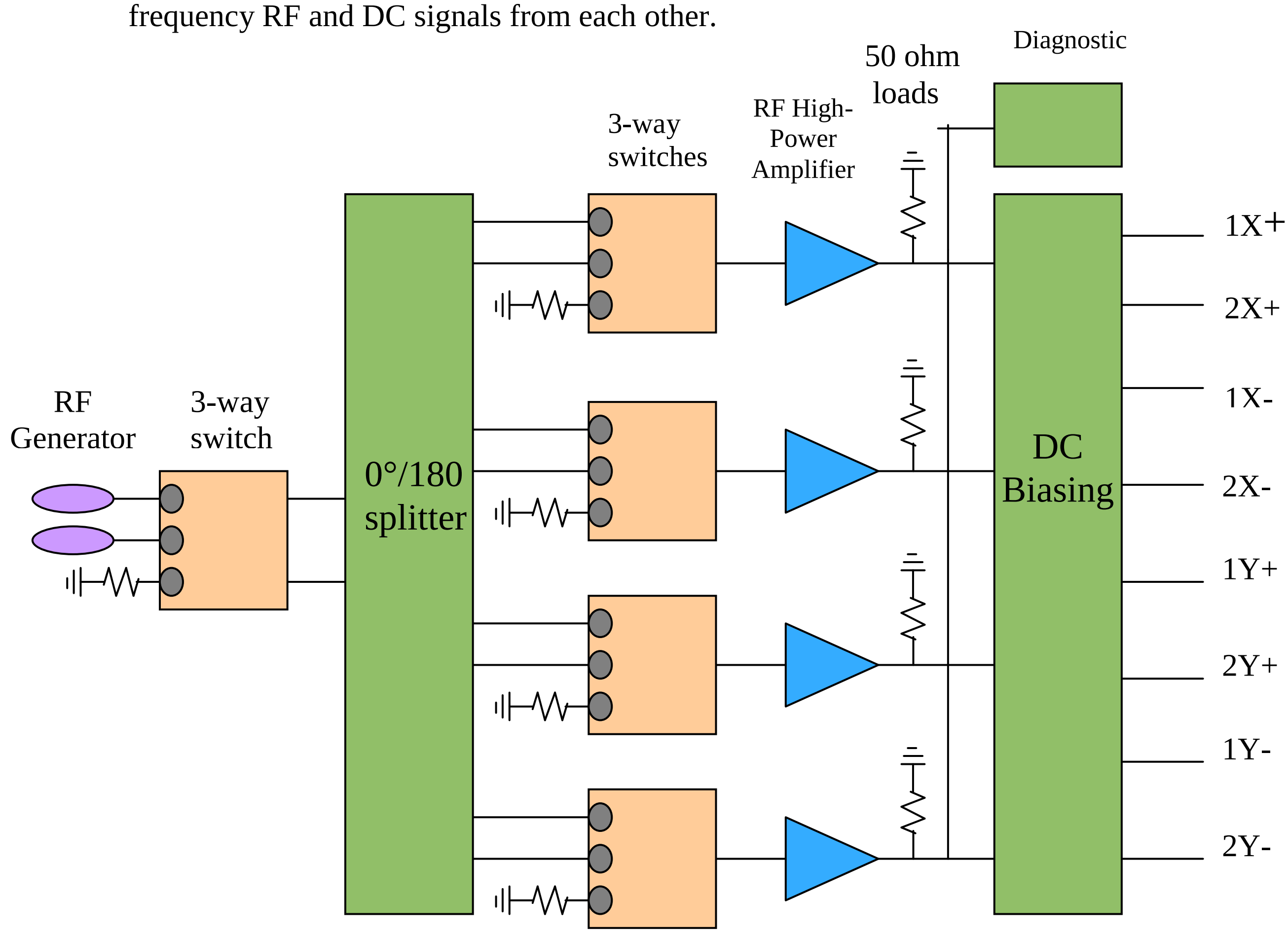


**Figure 4 – Diagram of MPET RF system**

# The EBIT

## 1. Motivation for Beta Spectroscopy

When the nuclear charge Z, of isobaric nuclei change by two units, the process is called $\beta\beta$-decay. It is believed that there exist at least two different modes in which this decay can occur; the $2\nu$-mode and the $0\nu$-mode. According to the Standard Model, the $0\nu$-mode is impossibility, since it requires that a neutrino be considered a Majorana particle.

In order to study $0\nu$ $\beta$-$\beta$-decay, it is necessary to have correct understanding of the $2\nu$ $\beta$-$\beta$-decay. To obtain a correct description of $2\nu$ $\beta$-$\beta$-decay process, single $\beta$ - and EC decay rates must be properly understood. It is believed that the elements in the EC decay rate matrix contain discrepancies of 1 or 2 orders of magnitude. The program to be implemented at TITAN aims to measure the EC branching ratios and hence correctly determine $\beta$-$\beta$- decay matrix elements. The advantages of doing this in an ion trap, as opposed to traditional methods of measurement, is that the traps provide an environment free of contamination. Possible candidates for the study of the EC ratios are $^{76}$As , $^{76}$Ge, $^{82m}$Br, $^{82}$Se, $^{100}$Tc, $^{100}$Mo, $^{110}$Ag , $^{110}$Pd, $^{114}$In ,$^{114}$Cd, $^{116}$In ,$^{116}$Cd, $^{128}$I , $^{128}$Te.

## 2. Description of EBIT and Beta Spectroscopy

The radioactive ion sample will be stored in TITAN's Electron Beam Ion Trap (EBIT), and monitored by seven X-ray detectors, which will be mounted near the center of the trap. The super-conducting 6T magnetic field, and electrostatic potentials applied to the trapping electrodes will trap the ions for several minutes. The figure displayed below shows that trap electrodes provide the electrostatic well-shaped potential need to axially trap the ions, while the two magnetic coils compress the beam's radius.

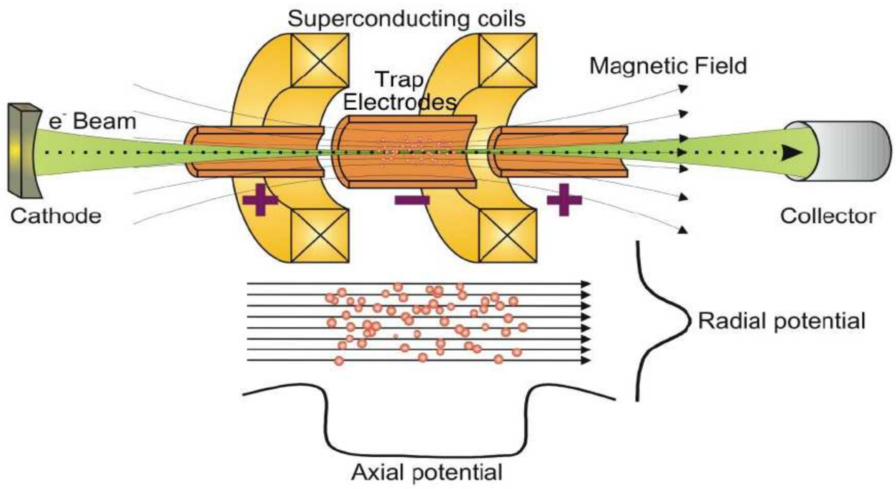


**Figure 5 – Electron Beam Ion Trap Diagram**

In the EBIT, the trapped ion cloud, which resembles a rotating spheroid is cooled using a buffer gas. Trapped ions colliding with the buffer gas results in a removal of energy from the ion cloud. The damping force felt by the ions results in changes to the original eigen motions of the ion cloud. The amplitude of the axial and reduced cyclotron motions decreases, while the amplitude of the magnetron motion increases. The instability of the magnetron motion leads to an expansion of the ion cloud, and a loss of outer ions as they hit the electrode plates.

The figure below how the size of the ion cloud changes as the density of the ion cloud increases, assuming that a 200V potential is applied to the end cap electrodes. Typically the ion cloud density is around the 0.45 $n_B$ mark. Because the whole in the end cap is only 2 mm wide, it is apparent that the ion cloud will have to be decreased.

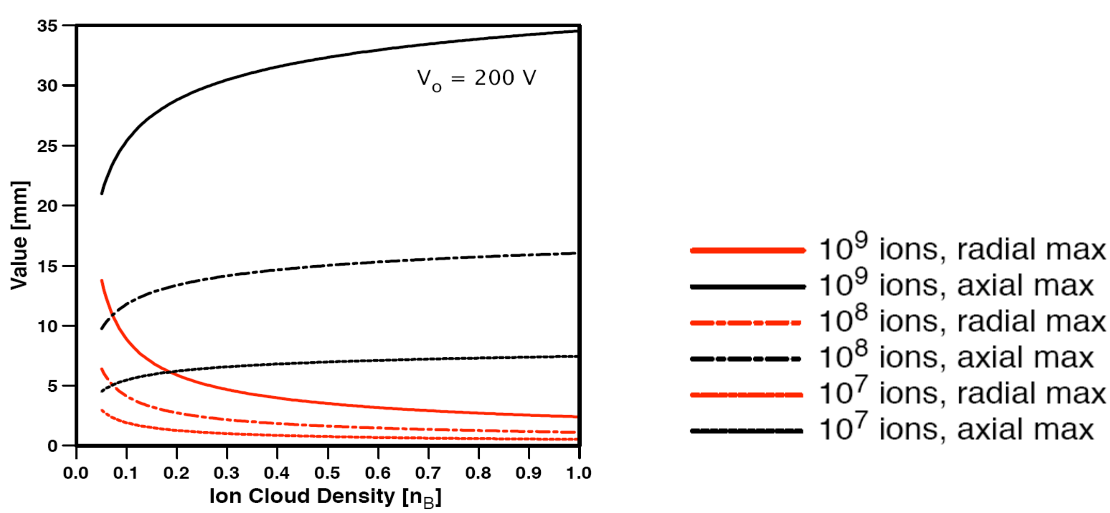


**Figure 6 – Relationship between ion cloud size and density**

## 3. Electrode Arrangement

The EBIT's had sixteen electrodes. Eight of these electrodes are grouped in fours and sit on either side of the central trap. These electrodes are named the collector side electrodes and electron gun side electrodes. Figure 7 shows their positioning.

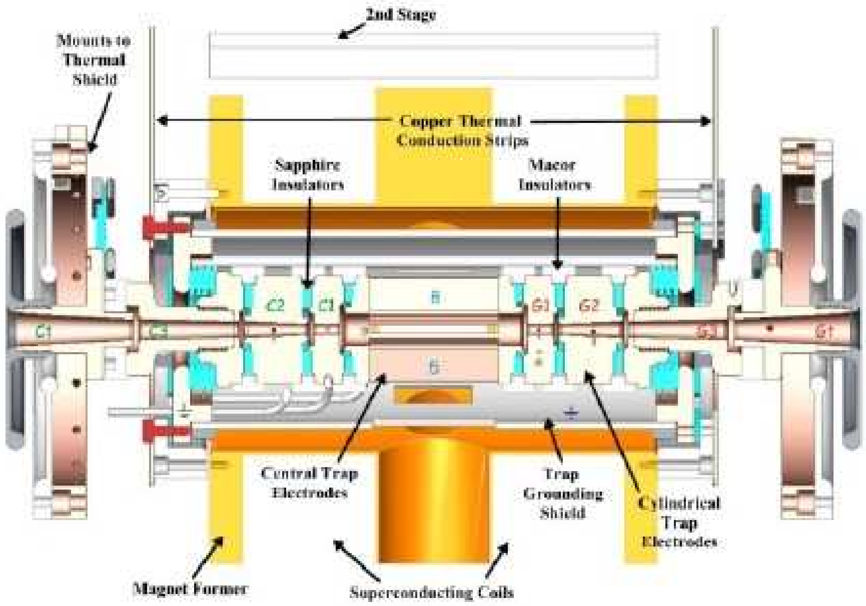


**Figure 7 – EBIT Electrode Arrangement**

The central trap consists of eight segmented electrodes numbered from one to eight in the counterclockwise direction. Figure 8 shows a diagram of what the central trap looks like. All of EBIT's electrodes can be biased independently. Radio frequency excitation may be applied to pairs of central trap electrodes in order to generate dipole and quadrupole configurations.

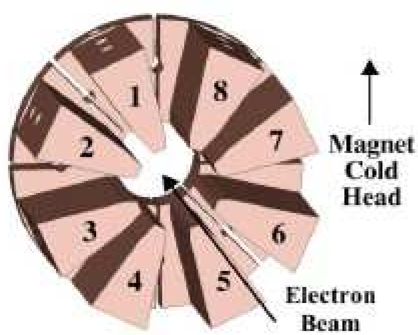


**Figure 8 – EBIT Central Trap Electrodes**

## 5. RF System Summary

### *A. Sideband Cooling*

For lower densities, sideband cooling is the preferred technique to compress the ion cloud. The magnetron motion ($\omega_-$) is controlled by coupling it to axial ($\omega_+$) or cyclotron ($\omega_c$) motions, using azimuthal quadruple RF fields. The ions are excited at a frequency equal to the sum of the frequencies of the coupled eigen motions. For sideband cooling, the following condition must be satisfied:

$$\frac{V_{\mathrm{RF}}}{2a^2} \geqslant B\delta. \qquad (1)$$

In the above equation, the parameter a is a good approximation to the inner diameter of the segmented central trap electrode, and $V_{RF}$ corresponds to the voltages that are applied to the neighboring segments. Sigma is a cooling parameter modeled by the equation

$$\delta = (q/mk_0)*( PT_0/P_0T) \qquad (2)$$

where $k_0$ is the reduced on mobility in a gas. Given these relationships, it can be seen that adjusting the pressure in the trap controls the voltages applied to the central electrodes, $V_{RF}$.

The advantage of coupling magnetron and reduced cyclotron motions is that the frequency is independent of the trapping potential, which is why simulations were performed using this technique. Given that equation (1) is satisfied, the resulting ion motion resembles a periodic exchanging of amplitudes between the magnetron and reduced cyclotron modes. Figure 9 shows the periodic conversion of magnetron motion to cyclotron motion.

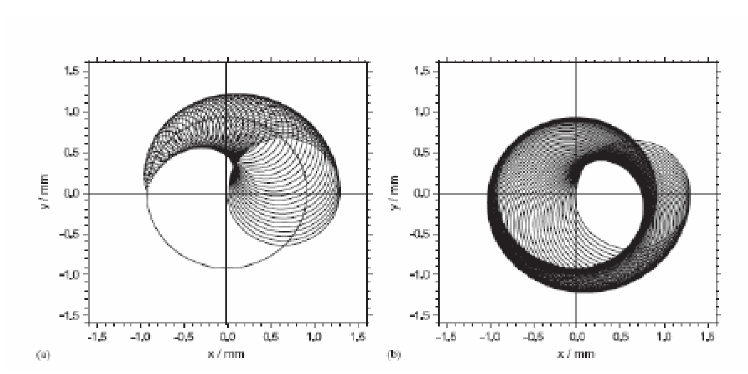


**Figure 9 – Coupled Magnetron and Cyclotron Motion**

Simulations done by Ryan Ringle, show that sideband cooling would be affective in the EBIT. Figure 10 shows what happens to the radius of $10^8$ ions when a 300V base-to-peak amplitude is applied to the central trap electrode. The end cap electrodes are set to 200V, and the simulation is run for 7.4 x $10^{-4}$ seconds. The parameters $r_0$ and $z_0$ represent the radius and axial length of the initial ion cloud respectively. It is apparent that the maximum ion cloud compression is achieved at a frequency of 1.2 the value of the sum of the coupled frequencies. This value is not exactly one due to the space charge effects present in a large ion cloud.

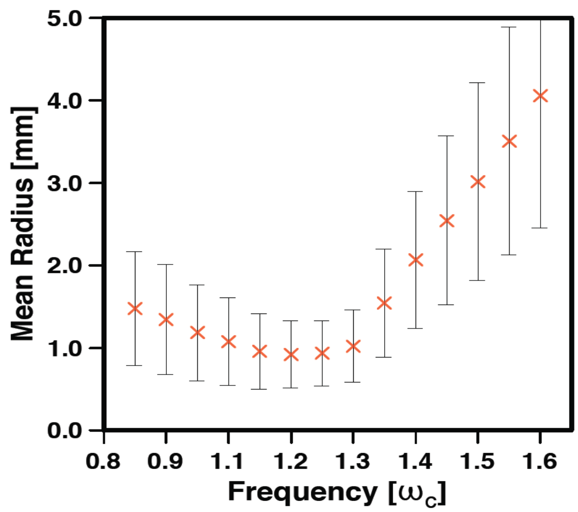


| | |
|---|---|
| Simulated ions | 1413 |
| Stored ions | $10^8$ |
| Reduced mobility | $1.86^{-4}$ ($Kr^+$ in He) |
| Gas temp [K] | 4 |
| Gas pressure [mbar] | $10^{-3}$ |
| $r_o$ [mm] | 5 |
| $z_o$ [mm] | 5 |
| Mass [A] | 80 |
| RF amp [V] | 300 |
| Sim. time [s] | $7.5 \times 10^{-4}$ |
| $V_o$ [V] | 200 |

**Figure 10 – Size of Ion Cloud When RF applied**

Due to the low density, and almost negligible space charge potential, the ion-ion interaction can be ignored, and the final volume of the beam is then proportional to the buffer gas temperature.

## *B. Rotating Wall Cooling*

When working with higher ion densities, where space charge affects rather than buffer gas temperature are the key factor, rotating wall cooling is preferred. This technique involves applying rotating electrical multiple fields that drag ions around the trap axis, in order to compensate for the damping. Allowing the frequency with which the field rotates to exceed the frequency of the rotating ion spheroid leads to a compression of the ion cloud. In the past, most groups have used laser cooling in combination with rotating wall cooling. While radial cooling is applied, the excess energy is converted into longitudinal energy, and hence laser cooling is applied in this direction. Due to the absence of laser cooling in the EBIT, rotating-wall cooling would be difficult to achieve, because the energy dissipated by the ion cloud has nowhere to go. However, at CERN rotating wall cooling in combination with buffer gas cooling was successfully implemented.

Because of the high ion density, and resulting space charge potential the RF applied to the central electrode of the trap would no longer be the cyclotron frequency of a single ion, shifted by a small factor, as in the case of sideband cooling. The applied frequency will have to take into consideration the plasma density and plasma frequency. The plasma frequency is given by:

$$\omega_p^2 \equiv \frac{q^2 n_0}{\varepsilon_0 m} \qquad (3)$$

where $n_0$ is the ion density. The maximum ion density is given by the Brillouin limit:

$$n_{max} = \frac{B^2 \varepsilon_0}{2m}. \qquad (4)$$

By rearranging equations 3 and 4, and using the relationship

$$\omega_c = qB/m \qquad (5)$$

it can be shown that at the Brillouin density, the plasma frequency, $\omega_p$, is equal to the cyclotron frequency, $\omega_c$ ,divided by $\sqrt{2}$. Therefore the upper limit for the applied rotating wall cooling frequency

# THE RF SYSTEM

## The MPET

### 1. The RF Generators

The generators are Agilent 33250A arbitrary waveform generators, and are rated for up to 80MHz. The generators cannot be frequency-modulated and amplitude-modulated at the same time. This is why the amplitude is set prior to a run, and the frequency is externally modulated by signals from the control system.

### 2. 180 Splitter Module

#### *A. The Circuit Design*

The 180 degree splitter module has been hard wired in order to accommodate 4 output channels and generate dipole and quadrupole excitation. A conceptual diagram of the splitter module is shown in Figure 12. A detailed schematic of the system below can be found in Appendix A. There are two radio frequency inputs. The lower frequency is used for dipole excitation, while the higher frequency is used for the subsequent quadrupole excitation. Switching between the frequencies is accomplished by a Mini-Circuits HSWA2-30DR+ absorptive RF switch, which operates on a single supply voltage of 3V. The switch circuit diagram, Figure 11, shows how the switch directs current from a common RF channels into one of 2 output channels or a 50Ω termination, and vice versa. The status of the switch is shown on the LED lights on the front panel of the NIM module. The truth table for the switch can be found in the datasheets in Appendix A.

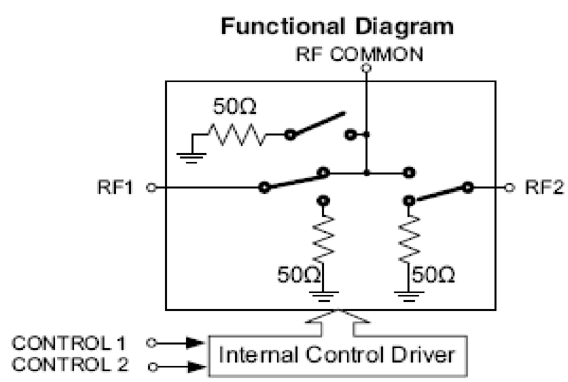


**Figure 11 – The Switch Circuit Diagram**

After the frequency selection, an AD8015 Wideband/Differential Output Transimpedance Amplifier from Analog Devices, serves as a 0° and 180° phase splitter. The amplifier provides a differential output as a function of input current, and is rated for up to 240MHz. A 50Ω resistor is shown on the splitter circuit diagram prior to the AD8015 input. This 50Ω resistor was replaced by two 25Ω resistors in order to attenuate the signal from 0.8V to 0.4V. With this configurations the optimum signal to noise ratio is achieved when a 1.4V peak-to-peak voltage is applied to the J9 and J10 inputs. This also corresponds to a 1.4V output. This output is too much for the amplifiers to handle, which is why a –6dB attenuator will be placed before the amplifiers.

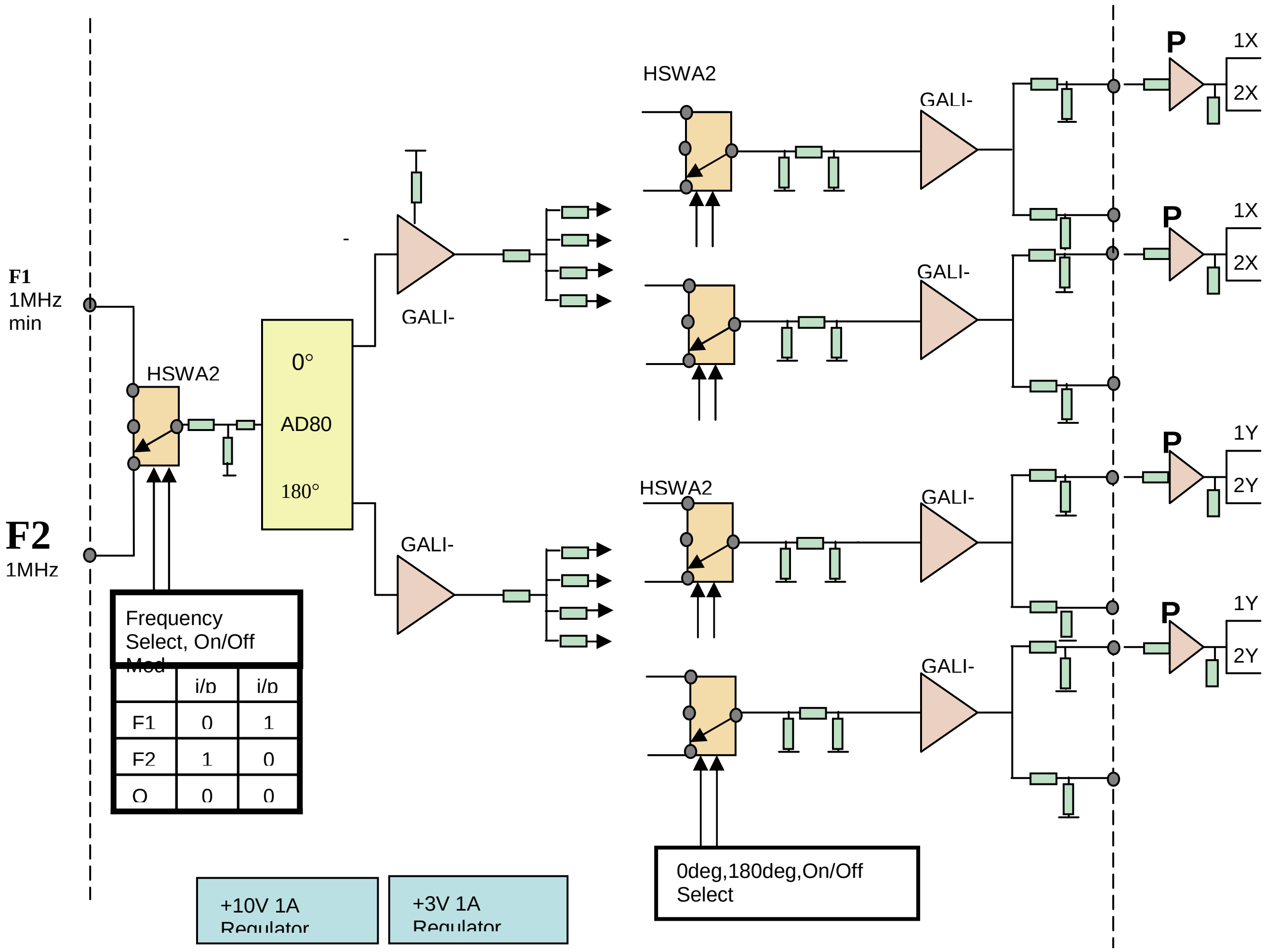


**Figure 12 – Schematic of 0°/180° Splitter**

A low -power monolithic Gali 51+ RF amplifier from Mini-Circuits then amplifies the signal on each channel. According to the datasheets, found in Appendix E, the Gali 51+ is specified for a DC to 8GHz frequency range and has a typical gain of 18.2dB.

The 0° and 180° signals are both split into 4 channels connected to 4 HSWA2-30DR+ switches. These switches are then able to select either the 0° signal, the 180° signals, or select the 50Ω termination resulting in no signal, in order to select the appropriate voltages and phases that need to be applied to each of the electrodes for the dipole or quadrupole settings.

The four resulting channels are once again amplified by the Gali-51+ amplifiers and split into 8 channels. Four of the channels connected to electrodes. Each connected channel leads to corresponding electrodes. The first output, depicted by J1, on the schematic, connects to electrodes 1X+ and 2X+. The J3 output lead to electrodes 1X- and 2X-, while the J5 and J7 outputs correspond to 1Y+/2Y+ and 1Y-/2Y- electrodes respectively. There are four channels that are not connected to electrodes. The unused channels may be used to analyze the signal while the system is running.

.

## *B. The Mechanical Setup*

The splitter boards sits inside of a NIM module. A list of parts required to assemble a NIM module can be found in Appendix A. The NIM module sits inside a NIM box which provides it with a +12 V power supply. The RF inputs and outputs are SMA jacks, and the TTL logic inputs for the switches are LEMO jacks. The digital logic of the system is described in subsequent sections. There are 3, green, 2mm, 570-0100-222F LED's from Dialight located on the front panel of the NIM module.  The LEDs indicate the switching status of the first switch, and are driven by a 74LCX14 hex inverter.

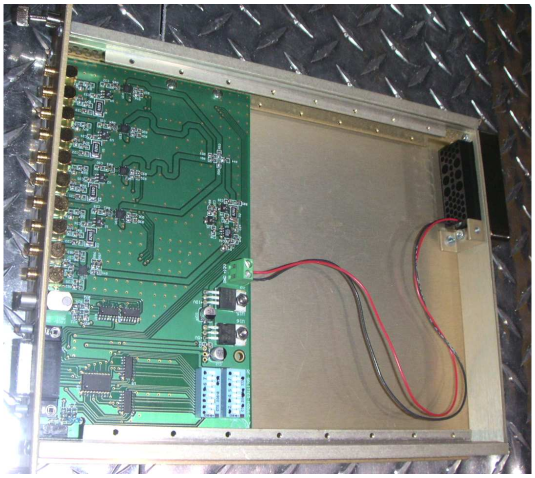

**Figure 13 – Splitter Circuit Board in NIM Module**

## *C. The Digital Logic*

The input signals come from a computer, connected to the module through 2-way LEMO connectors located on the front panel. One of the input signals dictates the on/off time modulation. The time modulation is necessary because the RF must be turned on once the ions are loaded into the trap and turned off before they are ejected. The excitation time, or pulse width, depends on the half-life of the isotope trapped, and can vary from 1ms to 10s. The signals on the second LEMO connector are responsible for selecting the frequency and the pattern, which dictates weather a dipole, or quadropole configuration is selected.

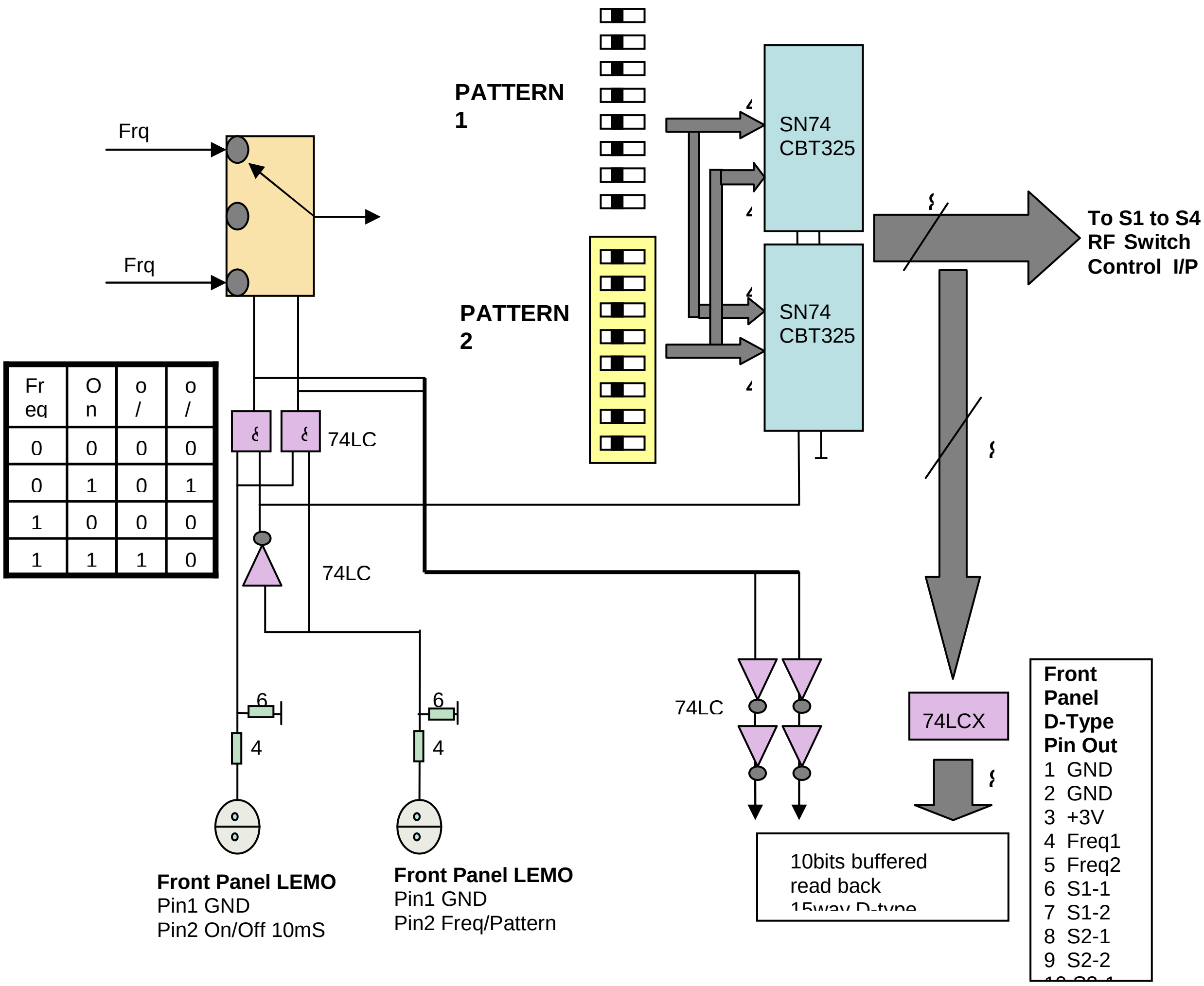


**Figure 14 – Digital Logic Schematic**

The status of first HSWA2-30DR+ switch, which selects the frequencies, is dictated by a 74LCX08 AND gate. The LCX08 contains four 2-input AND gates, which tolerate voltages up to 7V. The truth table in Figure 14 shows how the AND gate behaves. A high output (1) on the second channel results when the input from the *on/off* channel is high. A high output on the first channel results when the input from both the *on/off* channel and the *frequency select* channel is high. All other combinations of inputs result in a low (0) output on both channels. Connected to the AND gate, is a LCX14 hex inverter, from Fairchild, which transforms slowly changing input signals into sharply defined, jitter-free output signals. The inverter has 5V tolerant inputs.

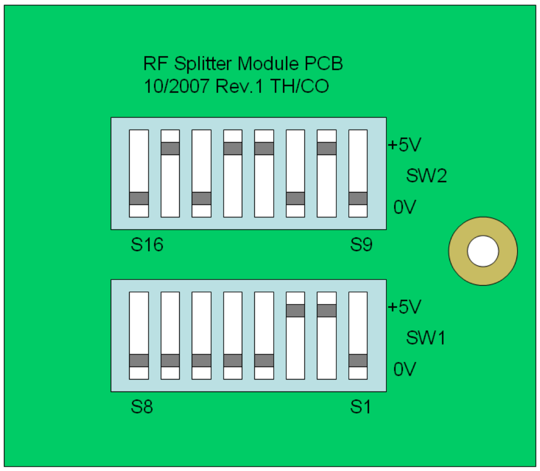


**Figure 15 – Switch Configuration**

The remaining four HSWA2-30DR+ RF switches are controlled by a 206-8ST DIP switches from CTS. The settings on the first switch, depicted by SW1 in the schematic, allow for a configuration that corresponds to dipole excitation. The settings on SW2 arrange the HSWA2-30DR+ switches in a way that make quadrupole excitation possible. Figure 15 shows in what position both switches must be in order to ensure that a dipole and quadrupole configuration is applied to the electrodes. Switching between these two patterns on the switches is accomplished through the SN74CBT3254 4-bit, 1-of-2 mutliplexer/demutliplexer from Texas Instruments. This device is connected to the second LEMO connector, and receives input from pattern select configuration. Detailed charts describing the implemented logic can be found in Appendix A.

# 3. RF Amplifiers

## *A. Specifications*

The four amplifiers are KMA1020M11models from Amplifier Research. They are class A amplifiers with a 25W power rating, and 100kHz -70Mhz frequency range. At an input power of 1mW, the maximum output power of 25W is achieved. The input and output impedance is 50Ω, and the output mismatch tolerance is 3:1. This means that operators must ensure that the amplifier outputs are terminated in 50Ω before the amplifiers are turned on. The steps required to turn on the amplifiers can be found in Alexei Bylinkii's August 2007 report.

Tests performed on the amplifiers showed that over the specified frequency range the gain flatness was within ±1.5dB. During the tests it was noted that the gain changes with temperature, and that there is very little gain compression towards the maximum rated power.

## *B. Gain Control*

Tests performed on the amplifiers showed that the amplifiers do not have the same gain within the 1% requirement. A gain control circuit was designed to in order to balance the gain on the channels. The gain control circuit allows operators to manually change the voltage on a PIN-DIODE attenuators which are built into the amplifiers. Adjusting the PIN-DIODE attenuators results in different gain values. Figure 16 shows a picture of the gain control circuit. The circuit contains 3266 trimming potentiometers from Bourns. The datasheet can be found in Appendix E. The circuit was placed inside an aluminum box and mounted onto the upper bar of the amplifier case.

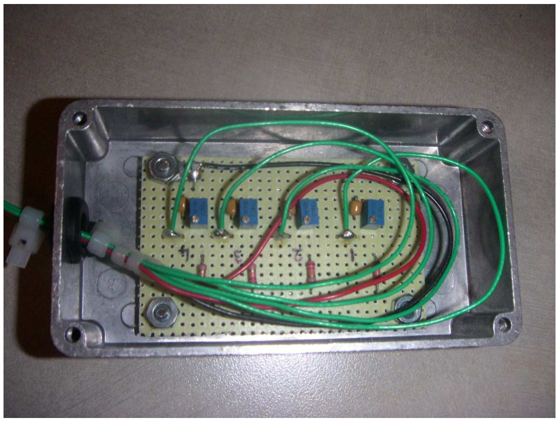

**Figure 16 – Gain Control**

## *D. Thermal Precautions*

The amplifiers may be damaged by the heat they generate. Keeping the amplifier case below 60°C prevents amplifier damage due to overheating. For this reason, the amplifiers are mounted onto heat sinks and cooled by 340 CFM fans. The fans can be found at TRIUMF stores, part #3-1/01002. Previous tests showed that with fan cooling the temperature of the amplifier case can be kept at about 30°C.

## *C. Power Supply*

The amplifiers are powered using an external 30V-10A power supply from Xantres. The datasheet for the HPD30-10GPIB model can be found in Appendix D. Tests on the amplifiers showed that each one draws below 5A from the power supply. For this reason, two power supplies are used to power all four amplifiers and their gain control circuits.

## *E. Mechanical Setup*

The amplifier case is shown in Figure 17. It is located in the cabinet next to the railing across from the penning trap. The gain control circuit box sits in between the amplifiers. Mechanical drawings of the case can be found in Appendix C.

**Figure 17 – Amplifier Case**

## 4. Terminations

The RF signal from the amplifiers is terminated into 50Ω. The terminations are four 50Ω resistors rated for 100W. Past tests have showed that when measurements were made with a network analyzer, the match was confirmed to be 50±2 Ω across the frequency range. The maximum reflected power was –35.5Db at 42MHz. The resistors heat up to approximately 72°C, which is why they are mounted on a circuit board that sits on a heat sink and is cooled by fans. More information on tests performed on the resistors can be found in Alexei Bylinskii's August 2007 report.

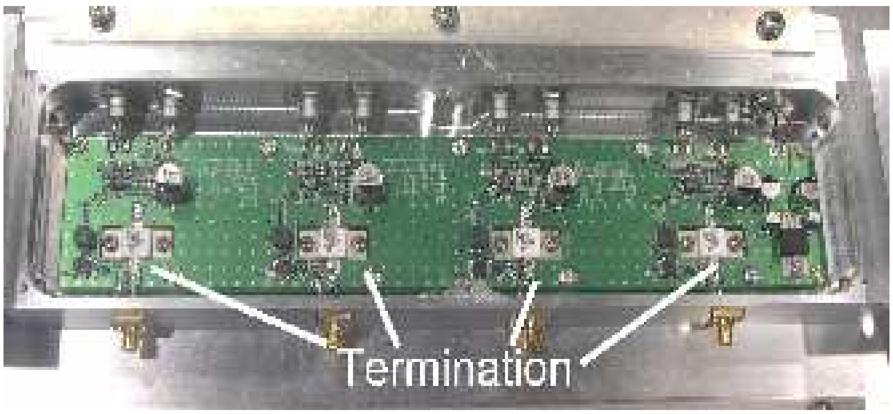


**Figure 18 – Terminations**

As shown in Figure 18, the terminations are connected to the peak diagnostic detectors described in subsequent sections.

## 5. Peak Diagnostic Detector

### *A. The Circuit Design*

The peak diagnostic detectors provide information about the RF amplitude on the guard electrodes. They allow users to monitor the system, and inform them of system failure. They also provide the information needed to balance the RF amplitude on different channels. A schematic of the detector is shown in Figure 19.

The SD101AW silicon schottky diodes have a low forward voltage drop of 0.6 V, and very fast switching action. The BAS70E6327 diodes from Infineon Technologies are rated for 70V.

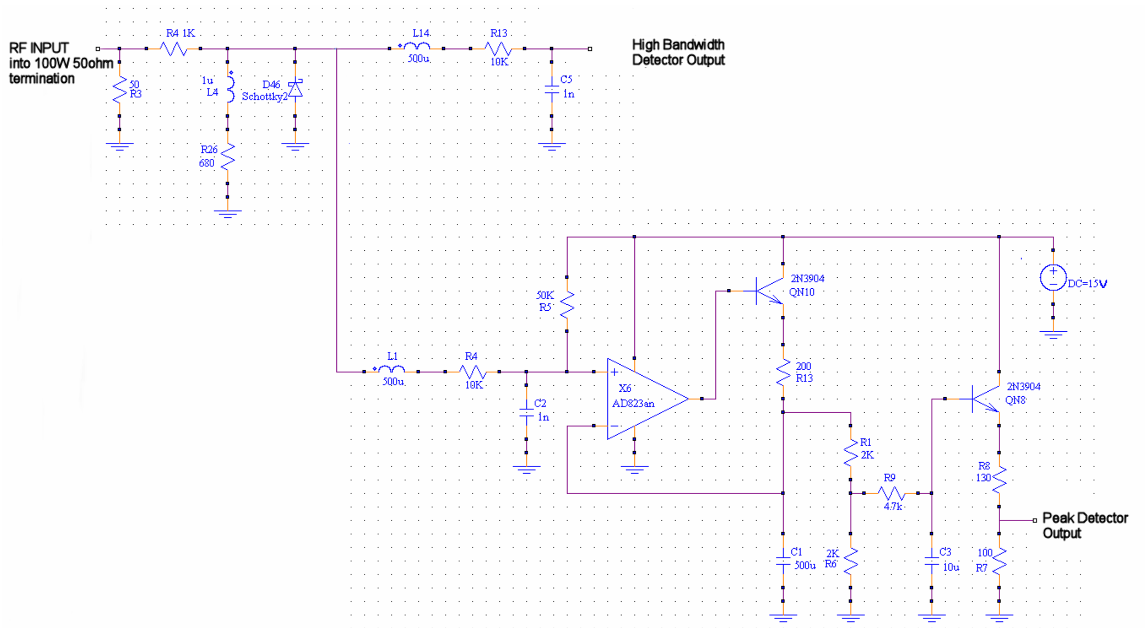


**Figure 19 – Diagnostic Detector Cir cuit**

A TUSONIX 4400-034 filter capacitor is used as the power input for the circuit. A LM2940ct-15/NOPB voltage regulator from National Semiconductor, rated for 1A and 15V, is used to regulate the voltage. The ground is connected to a plate that is mounted onto the inside of the box by the capacitor.

## *B. Mechanical Setup*

The outputs of the four peak diagnostic detectors are connected to 2-way LEMO connectors. Six of the connectors are connected to a cable that is plugged into the computer. The two remaining channels are connected to the scope using an SMA to BNC adapter from Newark. The cable used is a 2 way, 28 AWG, shielded cable, 3-5/02002 from stores.

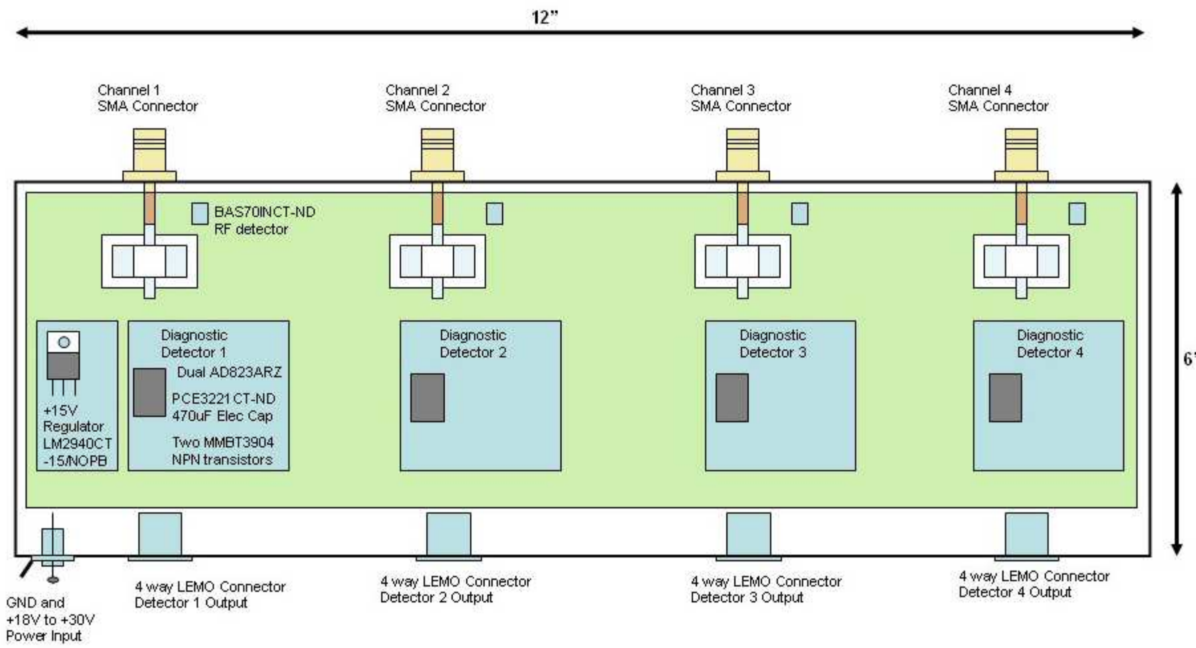


**Figure 20 – Diagnostic Detector Mechanical Setup**

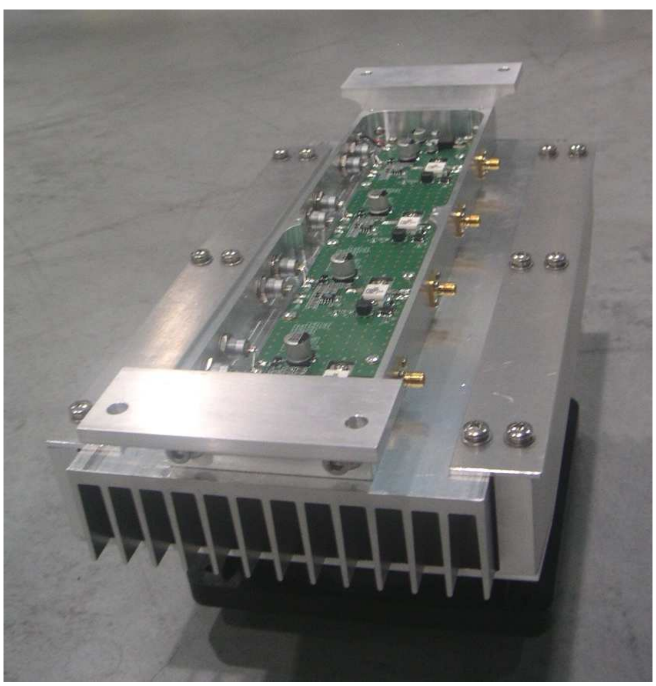

The peak diagnostic detectors circuit board, and the terminations are mounted into a custom-made aluminum box. The box specifications can be found in Appendix C. The setup sits on a heat sink and is cooled by a 430 CFM fan from TRIUMF stores (part # 3-1/01002). A picture of the entire setup is shown in Figures 20 and 21.

**Figure 21 – Diagnostic Detector case.**

## 6. DC Biasing Module

### *A. The Circuit Design*

The circuit board for the DC biasing module has 8 chancels, and each corresponds to one electrode. A circuit diagram for one channel is shown in Figure 22. The parts for the circuit board were chosen by using PSPICE simulations. Details of the simulations can be found in Alexei Bylinskii's August 2007 report.

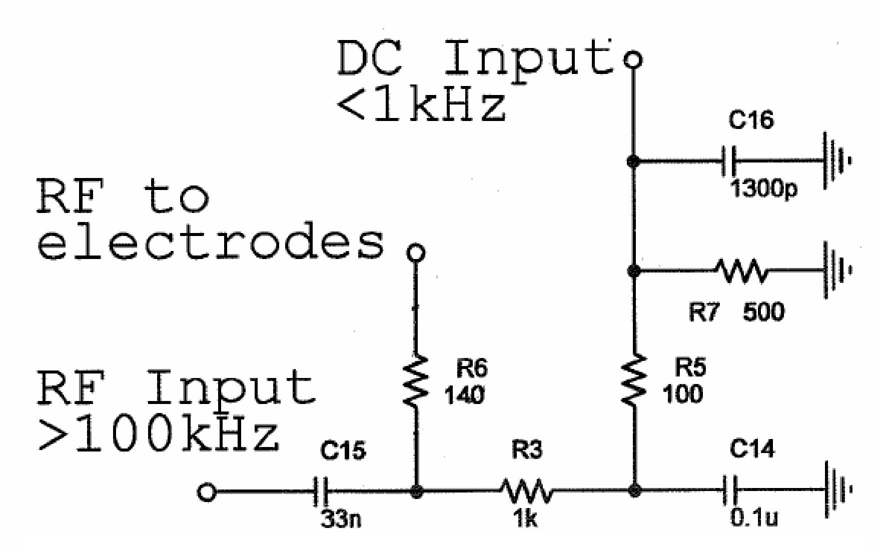


**Figure 22 – DC Biasing Module Circuit**

The channel which provides the DC input has a low pass filter which passes all frequencies below 1 kHz and attenuates signals above 10kHz. The filter is needed because of the 1300pF capacitance caused by the D-sub connector used for the DC inputs. The RF input has a 33nF capacitor beside it, which allows frequencies above 100kHz to pass untenanted.

There are 120Ω resistors in the DC biasing module. One end of each resistor is soldered to the PCB board, while the other end will be connected to the feed-through pins with set-screws. The resistors correct the voltages at the electrodes. The RF voltage on the actual electrodes does not always correspond to the voltages read off by the peak detector. A test setup was used to find out the relationship between the voltages at the terminations and at the actual electrodes. A 120Ω , 3 W placed in series with the RF path makes up for the discrepancy between the two voltages. The resistor also attenuates the reflected power.

*B. The Mechanical Setup*

The circuit board sits on one-inch stands attached to the upper lid of a cylindrical shield. The upper lid contains 8 SMA jacks for the RF inputs. Currently only four of the RF inputs are used in order to accommodate dipole and quadrupole excitation. The RF signal is transmitted to the inputs by means of a 50 Ω, RG 8X, double shielded coaxial cable from Belden. SMA male-female-male TEE pieces are used in order to connect the DC module to the terminations and diagnostic detector. SMA jack-to-jack adapters are used on one end of each TEE piece in order to connect the piece to the SMA plug at the end of the RG8X cables. A 9-way female D-sub is used for the DC inputs. The drawing for the lid and cylindrical shield can be found in Appendix D. A special cable was made for the DC inputs, with a male 9-way D-sub connector at one and 8 BNC plugs at the other end.

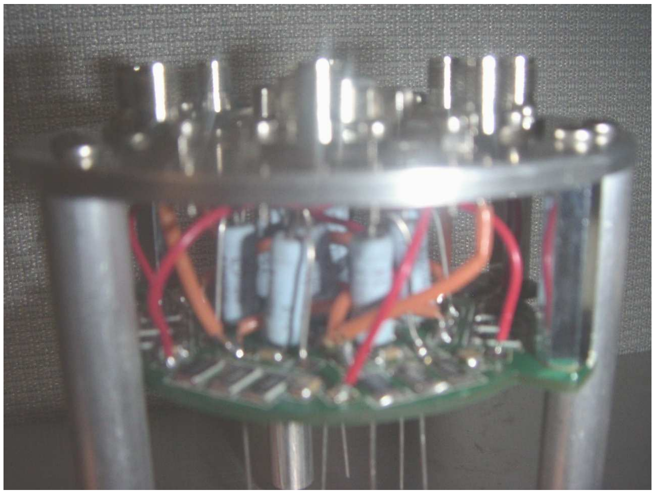

**Figure 23 – DC Biasing Module Mechanical Setup**

# The EBIT

## 1. Sideband Cooling Requirements

The following calculations were performed on the assumption that the ions in the trap are singly charged. The calculations were done for the range of ions for beta spectroscopy. In the future additional calculations may be done in order to take into account a greater range of ions. For detailed charts containing the calculations please refer to Appendix E.

| **Requirement** | **Reason** |
|---|---|
| 350 kHz- 125 MHz frequency range | The frequency range is calculated by figuring out the cyclotron frequency using the relation $\omega_c = qB/m$. The ion with the highest q/m ratio, hydrogen, gives the upper bound, while the ion with the lowest q/m ratio, singly charged uranium, gives the lower frequency bound. Due to the space charge effects in denser ion clouds, the actually frequency required, $w_{cool}$, will be shifted from the $w_c$ by some factor. Since the maximum number of ions trapped in the EBIT will be on the order of $10^8$, the cooling frequency $w_{cool}$ will not exceed $w_c$ x 1.25. |
| 1-100V applied to central trap electrodes | A lower bound for the voltage applied to the central electrode can be obtained by the relation $V_{RF} \geq 2Ba^2\delta$, where the cooling parameter depends on the ion mobility and adjustable pressure. The voltage range is so high because it is dependant on the EBIT pressure which can range from a typical value of 0.00001mbar to a maximum value of 0.001mbar. |
| | Because the ions are trapped in the EBIT for 100ms, the central electrode voltage will have to be switched on and off rapidly in order to ensure a short cooling time. The cooling period depends on the pressure in the potential minimum of the trap |
| Amplifiers will have to be floated at 5kV | See mechanical considerations |

## 2. Rotating Wall Cooling Requirements

The following calculations were done for the range of ions for beta spectroscopy. In the future additional calculations may be done in order to take into account a greater range of ions. For detailed charts containing the calculations please refer to Appendix E.

| **Requirement** | **Reason** |
|---|---|
| 350 kHz – 70MHz frequency range | Since $\omega_p = \omega_c/\sqrt{2}$, and $\omega_c = qB/m$, the highest frequency is obtained by calculating the cyclotron frequency of the ion with the highest q/m ratio, hydrogen. Taking a value of 6T for the B field, and calculating hydrogen's cyclotron frequency gives a value of 90MHz. Dividing 90MHz by √2 gives the upper frequency bound of 70MHz. Similarly, the lower bound is given by calculating the lowest q/m ratio, which is found in singly charged uranium. |
| 10 V applied to central trap electrodes | Although there is no concrete formula for obtaining an applied voltage range, 10 V is the experimental value obtained by most groups who have applied rotating wall cooling in similar situations |
| Amplifiers must be floated at 5kV | See mechanical considerations |

## 3. Mechanical Considerations

There are several considerations that need to be taken into account before commencing with the final design for the RF system. The schematic below illustrates how each of the eight, electrode, feed-through terminals will be changed to accommodate the RF system. The 5kV voltage source, shown in part A of the diagram, is floated on an additional 5 kV. Therefore, the voltage seen by the shielded cables leading to the electrodes (yellow), is 10 kV, meaning that an additional grounded shield (orange) must be built around the system for safety purposes. Also, in order to apply an RF voltage to the wires, the shielded cables encapsulating them must be reduced from the floating voltage to zero. Part B of the diagram shows what type of circuit might be necessary in order to accomplish this. Currently, the trap electrodes cannot be floated above 5kV because the grounded feedthrough before the first flange, depicted by C, is only rated for 5kV. In the future this feedthrough might be connected to the grounded shield (orange), and changed to accommodate a 20kV voltage. The first flange, depicted by C, would be floated at 5kV, and protected by a grounded shield. The last part of the diagram, shows that past the ceramic break, the second flange, is grounded. The eight electrodes will have to be connected in pairs in order to get azimuthal quadruple excitation.

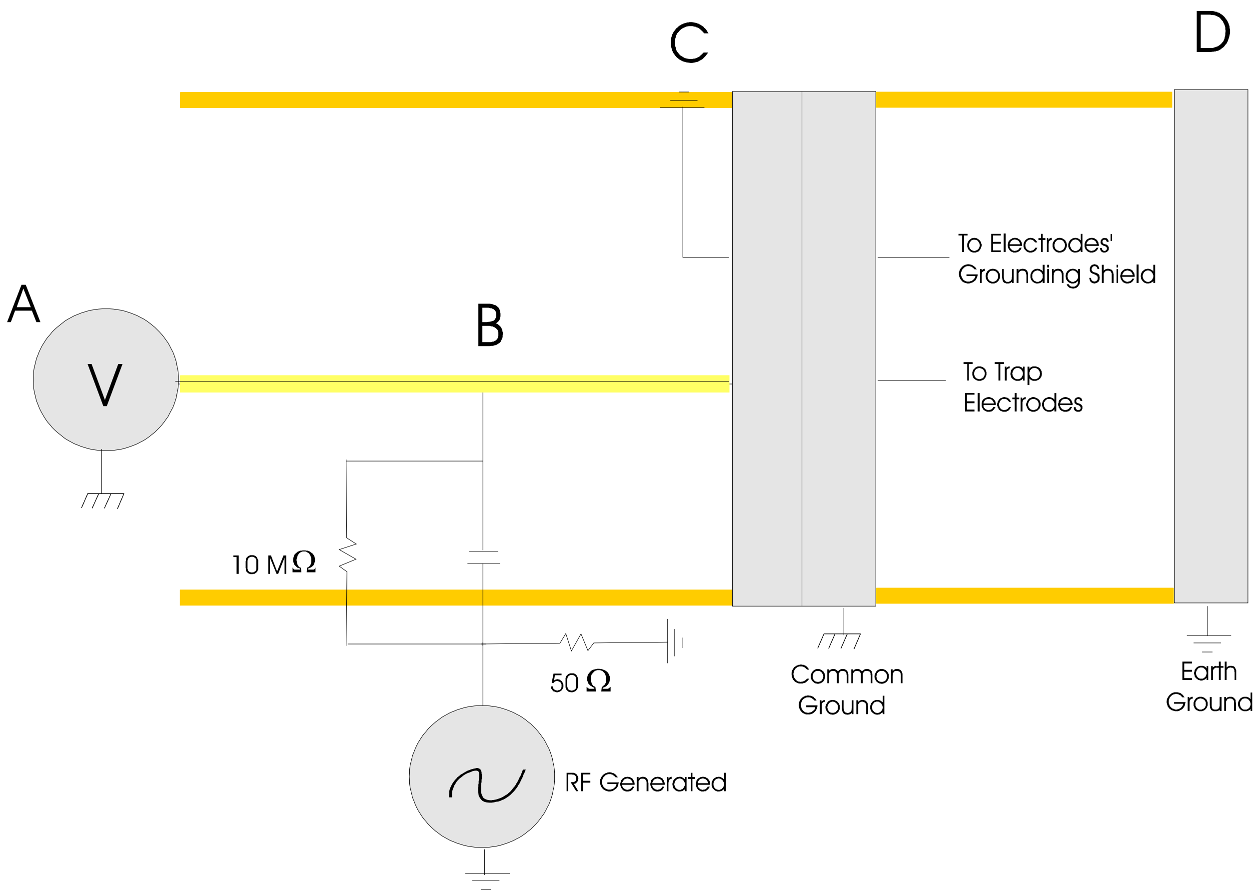


**Figure 24 – EBIT connections**

# CONCLUSION

## Current Status and Future Development

### MPET

For the MPET RF system most of the components are ready to be installed. The amplifier power supply, amplifier case and 12 V NIM box have been placed in the cabinet next to the railing by the penning trap. The amplifiers will arrive in January 2008, and be installed soon after that. The current 17 foot RG8X cables leading from the DC Biasing Module to the amplifiers will have to be made longer in order to fit in the cable tray that runs underneath the platform. The 6 foot cables from the Generators to the Splitter module will also have to be extended in order to accommodate the distance between the two devices.

The DC biasing module has been assembled and is ready to be connected to the trap. When connecting the resistors to the feedthrough pins, users will have to refer to charts and diagrams in Appendix B, in order to ensure that the electrodes get correctly hooked up to the RF inputs.

The splitter board has been placed inside the NIM module. The replacement splitter board is with Chris Owen. In the future if the replacement splitter board is needed, one more HSWA2-30DR+ absorptive RF switch and two surrounding resistors will have to be soldered on to it. Because the pads on the board were not made long enough in order to hand solder the switch, Chris Owen will need to use solder paste to connect it to the board. On the replacement board the 50Ω resistors before the AD8013 splitter will have to be replaced with 25Ω resistors. A NIM module will have to be assembled for the replacement board.

The diagnostic detector board has been assembled and placed inside its case. Once the new amplifiers come in, the detector will be placed underneath the penning trap, where the old amplifiers were. The cables leading from the diagnostic detector to the scope and data acquisition system will have to be assembled. The cable is a 28AWG, shielded cable purchased from stores. The required 2-way LEMO connectors and BNC have been handed off to Chris Owen.

## EBIT

Depending on the ion density in the EBIT, sideband cooling, rotating wall cooling or both will be implemented in future experiments. Sideband cooling would require a frequency range of 350 kHz to 125 MHz at 1 – 100 V applied to the central trap electrode. The voltage range is big because it varies with the EBIT pressure. Rotating wall cooling would require 350kHz – 70MHz at 10 V applied to the central Trap Electrodes.

The voltage and frequency calculations for cooling in the EBIT will still have to be verified. The current calculations take into account the ions needed for Beta Spectroscopy. Further calculations should be performed in order to take into account a greater range of ions that might be explored in other EBIT experiments.

Another motivation for the implementation of cooling in the EBIT is Fourier transform-ion cyclotron resonance mass spectrometry and should be further explored. Several papers on this subject can be found in the EBIT folders.

## REFRENCES


1. Froese, Mike. *The TITAN Electron Beam Ion Trap: Assemply, Characterization, and First Testes*, University of Manitoba, 2006.
2. D. Frekers, J. Dilling, I.Tanihata. *Electron Capture Branching Rations for the Odd-Odd Intermediate Nuclei in the Double-Beta Decay Using the TITAN Ion Trap Facility*, NRC Canada 2006.
3. F. Ames et al. *Cooling of Radiactive Ions with the Penning Trap REXTRAP*, 2004.
4. P. Beiersdorfer et al. Fourier Transform – *Ion Cyclotron Resonance Mass Spectrometry – A New Tool for Measuring Highly Charged Ions in an Electron Beam Ion Trap*, Elsevier Science, 1995.
5. Delheij et al. *The TITAN Mass Measurement Facility at TRIUMF-ISAAC*, draft
6. Bylinskii, Alexei, *The RF system for the TITAN Mass Measurement Penning Trap*, August, 2007
7. Ryjkov, Vladimir, *TITAN Penning trap DAQ/controls design*, October 13, 2005. TRIUMF
8. TITAN website, http://titan.triumf.ca
9. LEBIT website at NSLC, http://groups.nscl.msu.edu/lebit

# APPENDICES